

Alma Mater Studiorum Università di Bologna  
Archivio istituzionale della ricerca

Amine functionalised silicon nanocrystals with bright red and long-lived emission

This is the final peer-reviewed author's accepted manuscript (postprint) of the following publication:

*Published Version:*

Morselli G., Romano F., Ceroni P. (2020). Amine functionalised silicon nanocrystals with bright red and long-lived emission. FARADAY DISCUSSIONS, 222(0), 108-121 [10.1039/c9fd00089e].

*Availability:*

This version is available at: <https://hdl.handle.net/11585/786148> since: 2021-02-26

*Published:*

DOI: <http://doi.org/10.1039/c9fd00089e>

*Terms of use:*

Some rights reserved. The terms and conditions for the reuse of this version of the manuscript are specified in the publishing policy. For all terms of use and more information see the publisher's website.

This item was downloaded from IRIS Università di Bologna (<https://cris.unibo.it/>).  
When citing, please refer to the published version.

(Article begins on next page)

This document is the Accepted Manuscript version of a Published Work that appeared in final form in *Faraday Discussions*:

**Amine functionalised silicon nanocrystals with bright red and long-lived emission**

Giacomo Morselli, Francesco Romano, Paola Ceroni

*Faraday Discuss.* 2020, 222, 108-121.

© 2020 Royal Society of Chemistry (RSC) after peer review.

To access the final edited and published work see:

<https://doi.org/10.1039/C9FD00089E>

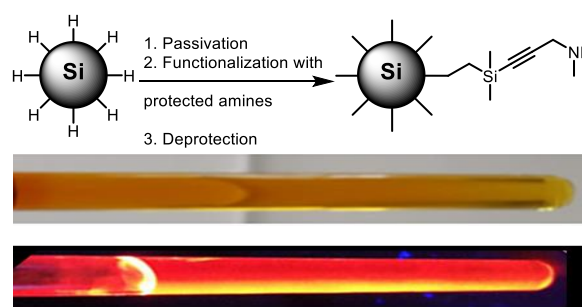
# Amine functionalised silicon nanocrystals with bright red and long-lived emission

Giacomo Morselli, Francesco Romano, Paola Ceroni

Department of Chemistry "Giacomo Ciamician", University of Bologna, via Selmi 2, 40126, Bologna, Italy, e-mail: [paola.ceroni@unibo.it](mailto:paola.ceroni@unibo.it)

## ABSTRACT

When functionalised with amines, silicon nanocrystals (SiNCs) are known to have surface-state emission with loss of colour tuneability, low quantum yield and short nanosecond lifetimes. The change in optical properties are produced by direct amine bonding on the silicon surface. In this article, secondary amine functionalised SiNCs with bright, red ( $\lambda_{\max}=750$  nm) and long-lived emission ( $\tau$  ca. 50  $\mu$ s) are reported for the first time via a three-step synthetic approach. These SiNCs are colloiddally stable in several polar solvents and can be further functionalised by reaction with carboxylic acid groups. We proved further functionalization feasibility with pyrene butyric acid: ca. 40 pyrene units per nanoparticle were attached via amide bond formation. The resulting hybrid system works as a light-harvesting antenna: excitation of pyrene units at 345 nm results in sensitised emission at 700 nm by the silicon core.



## INTRODUCTION

Silicon nanocrystals (SiNCs) are luminescent semiconductor nanoparticles that are a valid biocompatible alternative to conventional quantum dots.<sup>1-6</sup> Quantum dots are often made of elements of the group III-V and II-VI. The presence of elements like cadmium and lead prevents their use in consumer products or in biological applications. Silicon has advantages in these contexts since it is abundant on the Earth's crust, has a relative low cost and especially it is non-toxic.<sup>7</sup> Moreover, SiNCs display photophysical properties that render them interesting for several industrial and imaging applications: their emission spans from visible to near infrared spectral range according to their dimensions, and matches the optical window that most penetrates biological tissues. The emission quantum yield is reported to reach high values (up to 70%)<sup>8</sup> and their emission lifetimes are longer than those of direct bandgap quantum dots (tens or hundreds of microseconds). This last characteristic allows to use time-gated detection<sup>9</sup> in order to obtain a clean signal which is not influenced by the noise caused by the short-lived tissues' autofluorescence or by the back-scattered excitation light.<sup>10-12</sup>

However, their wide utilization is hindered, to some extent, by the following issues: commonly used passivating ligands, i.e. alkyl chains, prevent suspension of SiNCs in polar solvents; the molar

absorption coefficient in the visible range is inferior to that of molecules or conventional quantum dots because of the indirect bandgap nature of silicon.

Our group demonstrated that by decorating SiNCs' surface with chromophores their absorption coefficient is strongly enhanced in the UV and visible spectrum. Most importantly, these hybrid systems work as light-harvesting antennae: upon excitation of the organic dye, sensitised emission of the silicon core is observed by efficient energy transfer processes.<sup>13-15</sup> The brightness of the system (defined as the product between the molar absorption coefficient at the excitation wavelength and the emission quantum yield of the antenna) is significantly improved (up to 300%<sup>13</sup>). However, these antennae were obtained via competitive hydrosilylation reactions in which terminal olefin functionalised chromophores reacted together with a co-passivating ligand that was used also as a solvent. These reaction conditions together with high temperatures (180°C overnight) resulted in low chromophore loading on the SiNCs surface, despite the large excess used during the hydrosilylation step.

To circumvent this problem, it would be desirable to passivate SiNCs' surface with ligands containing terminal reactive groups that can be subsequently post functionalised under mild experimental conditions. Among the possible functional groups, amine-terminated SiNCs are ideal candidates because amide bonds can be formed by well-established amidation reaction, amide bonds are fairly stable under physiological conditions and a variety of derivatives are commercially available for amidation reactions. For example, this approach could lead to the functionalisation with visible absorbing chromophores, water-solubilising groups (e.g., PEG) or enzymes.

Amine functionalised SiNCs reported so far show blue PL, independent of the NCs size, attributed to surface defects introduced with the synthetic strategies employed.<sup>16-18</sup> Another applicable approach would be to use hydrosilylation of hydrogen terminated SiNCs obtained with thermal disproportionation of hydrogen silsesquioxane, with amine functionalised alkenes. Unfortunately, the interaction between the nitrogen atom of a primary or secondary amine and the silicon lattice can still compromise the typical optical properties of silicon nanocrystals,<sup>19</sup> suppressing the bright red long-lived photoluminescence (PL) and producing a blue short-lived emission with a lower quantum yield. Recently, a strategy based on borane protection was proposed to obtain amidine functionalised SiNCs with good photophysical properties that shows hydrophilicity switchable properties.<sup>20</sup> To the best of our knowledge, primary or secondary amine functionalised SiNCs with red emission and long lifetimes have not been reported.

In this paper, we discuss a synthetic route to obtain bright-red, long-lived emitting silicon nanocrystals functionalised with amines. This strategy consists of three steps: (i) passivation of SiNCs with chlorosilane via radical initiated hydrosilylation; (ii) functionalisation with amines protected by bulky groups; (iii) acid-induced deprotection of the amine functions. A post-functionalization through amide coupling was also successfully conducted with a very limited amount of pyrene, ca. 1.5% mol compared to previously published approach by our group.<sup>13</sup> The resulting system contains an average of 40 pyrene units per nanocrystal and works as an efficient light-harvesting antenna.

## EXPERIMENTAL SECTION

### Reagents and Materials

All reagents were purchased from Sigma-Aldrich and used without further purification if not stated otherwise. Dry toluene was obtained via distillation over calcium chloride under nitrogen atmosphere. N,N,N',N'-tetramethylethylenediamine was refluxed over fresh KOH and distilled under nitrogen. Nuclear magnetic resonance ( $^1\text{H-NMR}$ ) spectra were measured on an ARX Varian INOVA 400 (400MHz) spectrometer, chemical shifts are reported in ppm and data are reported as follows: chemical shift, multiplicity (s = singlet, d = doublet, t = triplet, q = quartet, br = broad, m = multiplet), coupling constants (Hz). GC-MS analysis were obtained using an Agilent Technologies MSD1100 equipped with EI (70eV) ionization system, single quadrupole analyser, and HP5 5% Ph-Me Silicon.

### Protection of N-methylpropargylamine with trityl chloride

In a 25 mL two-necked flask, under nitrogen atmosphere, 920 mg of trityl chloride (3.3 mmol, 1.1 eq), 7 mL of anhydrous dichloromethane (DCM), 450  $\mu\text{L}$  of anhydrous triethylamine (TEA, 333 mg, 3.3 mmol, 1.1 eq) and 255  $\mu\text{L}$  of N-methylpropargylamine (207 mg, 3 mmol, 1 eq) were added in this order. After several minutes, a formation of a precipitate occurred (the ammonium salt). The mixture was stirred at room temperature for 4 hours under inert atmosphere. The reaction was quenched with an aqueous solution of  $\text{NaHCO}_3$  and diluted with other 5 mL of DCM. The organic phase was washed twice with water, collected, dried with  $\text{Na}_2\text{SO}_4$  and concentrated at reduced pressure. TLC analysis (1:1 = cyclohexane:toluene as eluent phase) showed two spots ( $R_f = 0$ ,  $R_f = 0.8$ ) while developing with  $\text{KMnO}_4$ . The less polar one was identified as the product and separated with a flash chromatography using cyclohexane:toluene (1:1) as eluent phase. The collected fractions gave a white crystalline solid (673 mg, yield: 72%). GC-MS ( $m/z$ ):311.  $^1\text{H-NMR}$  ( $\text{CDCl}_3$ , 400 MHz),  $\delta$  (ppm): 7.0-7.5 (15 H, m); 2.93 (2 H, br s); 2.25 (3 H, s); 2.19 (1 H, t).

### Synthesis of Hydride-Terminated Silicon Nanocrystals (H-SiNCs)

Oxide embedded silicon nanocrystals were obtained via literature reported procedure.<sup>21,22</sup> Hydride-terminated silicon nanocrystals were liberated from the silica matrix through HF etching: 300 mg of oxide-embedded silicon nanocrystals were dispersed in a mixture composed of 3 mL of ethanol, 3 mL of bi-distilled water and 3 mL of a 49% solution of aqueous HF. (*Caution! HF is dangerous and must be handled with extreme care*). The mixture was stirred for 1h and 30 minutes under ambient light at room temperature. The nanocrystals were extracted with toluene (3x10 mL) and then centrifuged three times in toluene (8000 rpm for 5 minutes). Supernatant was discarded and the nanocrystals were then transferred in a dry box.

### Hydrosilylation of H-SiNCs with chloro(dimethyl)vinylsilane<sup>23</sup>

The nanocrystals were dispersed in 2 mL of dry toluene in an 8 mL vial. Two milligrams of 4-decyldiazobenzene tetrafluoroborate (4-DDB, about 6  $\mu\text{mol}$ ) were added. Afterwards, 400  $\mu\text{L}$  of chloro(dimethyl)vinylsilane (CDMVS, 3 mmol, 360 mg) were introduced to obtain chlorosilane-passivated silicon nanocrystals. The mixture was stirred overnight at room temperature. The mixture of chlorosilane-passivated SiNCs was then filtered, concentrated at rotary evaporator, transferred again in the dry-box and diluted in 2 mL of dry toluene.

## Functionalization of SiNCs with trityl-amines

In a two-necked 25 mL round-bottom flask, dried and filled with nitrogen, 180 mg of N-methyl-N-tritylpropargylamine (0.6 mmol) were introduced. The flask was transferred to a dry-box and 140  $\mu\text{L}$  of N,N,N',N'-tetramethylethylenediamine (TMEDA, 0.9 mmol, 105 mg) and 3 mL of dry toluene were added. The flask was then removed from the dry-box and plugged to a Shlenk line filled with  $\text{N}_2$ . After having cooled the reaction to  $-78^\circ\text{C}$  with a liquid nitrogen/acetone bath, 240  $\mu\text{L}$  of n-butyllithium (n-BuLi 2.5 M in hexanes, 0.6 mmol; *Attention: pyrophoric! It must be handled under inert atmosphere*) were added dropwise, while stirring. The acetone bath was removed after 45 minutes, and the mixture was stirred for 15 minutes at room temperature. Again at  $-78^\circ\text{C}$ , the suspension of silicon nanocrystals in 2 mL of toluene was slowly added to the reaction mixture. One hour later, the acetone bath was removed, and the reaction mixture was stirred for an hour at room temperature. Later, it was heated to  $40^\circ\text{C}$ , and stirred for another hour. The reaction was cooled again to  $-78^\circ\text{C}$  and a second amount of n-BuLi (120  $\mu\text{L}$ , 0.3 mmol) was added to complete the capping of the surface. The reaction was allowed to reach room temperature and stirred overnight. The introduction of 7 mL of MeOH made the nanocrystals precipitate. The brownish precipitate was washed 3 times with methanol and separated from the supernatant by centrifuge (8000 rpm, 5 minutes). The so obtained nanocrystals were dispersed in chloroform and the precipitate was filtered off.

## Cleavage of trityl group for ammonium-terminated silicon nanocrystals

The suspension of tritylamine functionalised silicon nanocrystals was transferred in a 20 mL vial with a magnetic stir bar and stirred slowly. Trifluoroacetic acid (TFA, 99%) was added dropwise carefully until the precipitation of silicon nanocrystals occurred (about 10  $\mu\text{L}$ ) due to protonation of amines. The suspension was let stirring for 10 minutes. Then it was centrifuged, washing three times with chloroform (3x8000 rpm, 5 minutes) and the precipitate was dissolved in alcoholic solvent (ethanol, methanol), acetonitrile or N,N-dimethylformamide (DMF).  $^1\text{H-NMR}$  and ninhydrin test before and after the deprotection confirmed the fading of trityl group (*Figure 1* and *2*). In the NMR spectrum, the signals related to the attached ligands are broadened because the motion of the molecules linked to the nanocrystal is hindered, resulting in a longer relaxation time.<sup>23,24</sup> The signals of trityl group lay between 6.7 and 7.7 ppm (*Figure 1a*); these signals are completely absent in the deprotected sample (*Figure 1b*). Ninhydrin test is an assay used to detect the presence of amines. Primary amines react with ninhydrin yielding a blue-coloured compound, secondary amines produce an orange compound and tertiary amines don't react.<sup>25</sup> The tritylamine functionalised SiNCs did not display a colour change when exposed to ninhydrin assay (*A* in *Figure 2a*), as expected for a tertiary amine functionalization of the surface (see e.g., N-methyl-N-tritylpropargylamine, *B* in *Figure 2a*). On the other hand, the deprotected SiNCs (*E* in *Figure 2c*) showed a yellowish color, similar to that of N-methylpropargylamine (*F* in *Figure 2b*), suggesting the presence of a secondary amine.

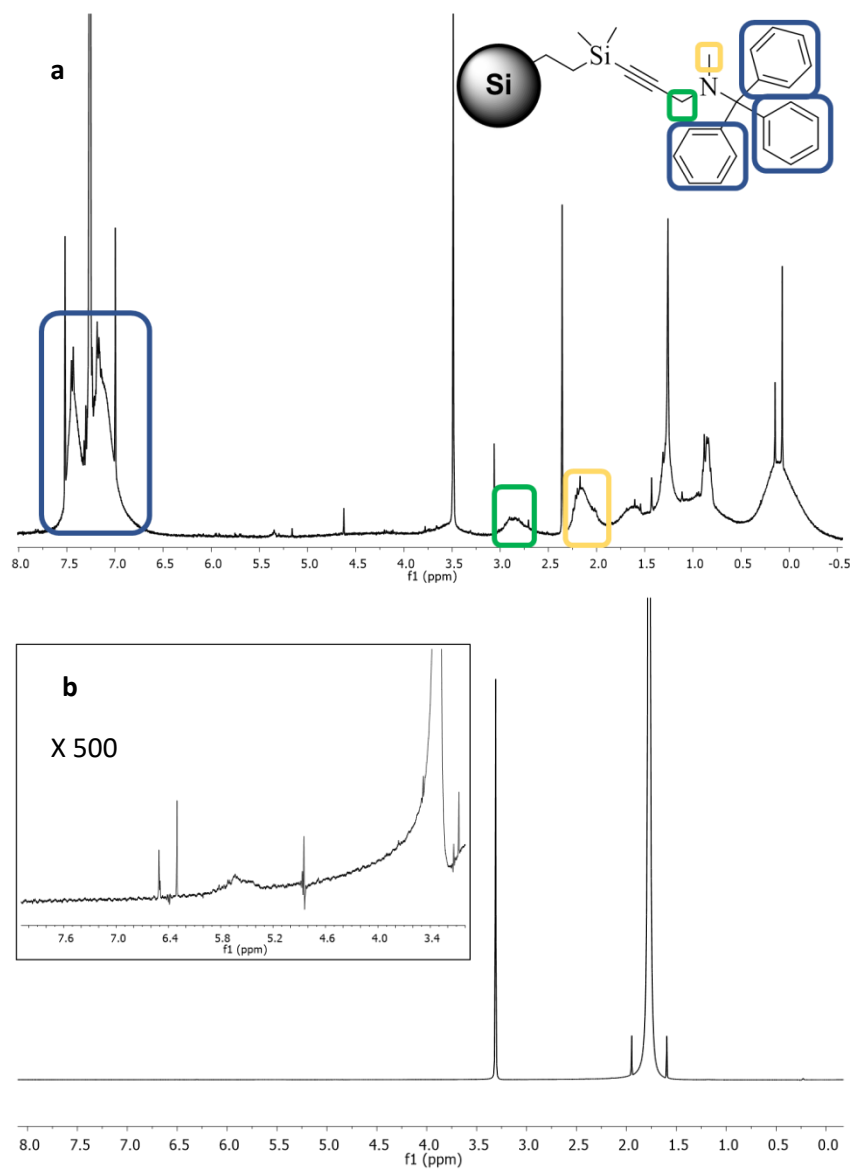


**Figure 1** – NMR spectra of (a) trityl functionalised silicon nanocrystals (400 MHz, CDCl<sub>3</sub>) and (b) ammonium functionalised silicon nanocrystals (400 MHz, CD<sub>3</sub>OD), with a 500x magnification in the inset, showing the absence of the aromatic signals

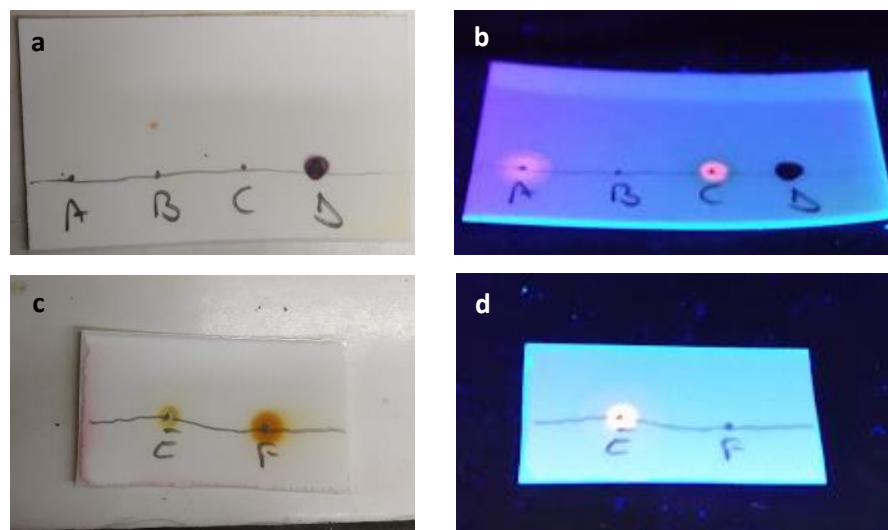


**Figure 2** – Ninhydrin test (a, b, c) on TLC plates for different suspensions: (A) tritylamine functionalised silicon nanocrystals, (B) a tertiary amine (here, N-methyl-N-tritylpropargylamine), (C) alkyl-passivated silicon nanocrystals (non-containing amines), (D) a primary amine (in this case, bis-aminopropyl polyethylene glycol), (E) amine functionalised silicon nanocrystals (after trityl cleavage) and (F) a secondary amine (N-methylpropargylamine), under visible (a, c) or 365 nm UV (b) light (picture d was taken before the test, to show the luminescence of the sample E under UV light)

Addition of triethylamine made the nanocrystals precipitate in ethanol and we could suspend them in chloroform because of the deprotonation of ammonium groups.

#### **Water-suspendable ammonium-terminated silicon nanocrystals**

An excess of a HCl solution in methanol was added to a suspension of silicon nanocrystals in methanol. An excess of water was then introduced, and the suspension filtered through 0.45 micrometres cut-off RC filters. The suspension was concentrated at rotary evaporator to remove methanol and the acid in excess.

#### **Amide coupling with 1-pyrenebutyric acid**

In a two-necked 25 mL round-bottom flask, under nitrogen atmosphere, 7 mg of 1-pyrenebutyric acid (0.028 mmol) were dissolved in anhydrous DMF. Then, 9  $\mu$ L of triethylamine (0.066 mmol, 6.6 mg), 5  $\mu$ L of 1-ethyl-3-(3-dimethylaminopropyl)carbodiimide (EDC, 0.03 mmol, 4.4 mg) and 13 mg of (1-cyano-2-ethoxy-2-oxoethylideneaminoxy)dimethylamino – morpholino – carbenium hexafluorophosphate (COMU, 0.03 mmol) were added. The suspension was let to stir for half an hour at room temperature. Half a batch of ammonium-terminated silicon nanocrystals derived from the etching of 300 mg of silica-embedded SiNCs, dispersed in 2 mL of DMF was added to the mixture, which was then let stirring for 1 hour and a half. Therefore, other 5  $\mu$ L of EDC and 13 mg of COMU were added, and the mixture was let stirring overnight. The addition of several mL of methanol made the nanocrystals precipitate. They were centrifuged five times with methanol (8000 rpm, 5 minutes) and the supernatant dispersed in DMF.

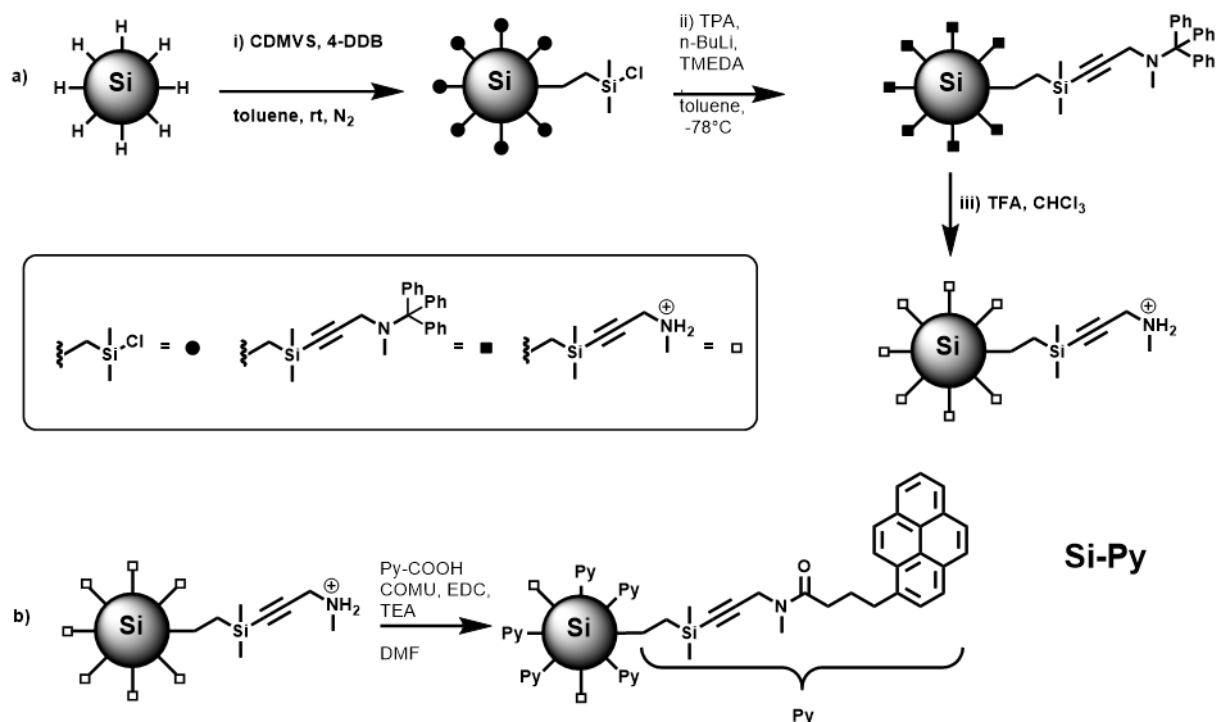
## Photophysical measurements

Photophysical measurements were carried out in air-equilibrated ethanol, chloroform, water or N,N-dimethylformamide at 298 K. UV-visible absorbance spectra were recorded with a Perkin Elmer  $\lambda$ 650 spectrophotometer, using quartz cells with 1.0 cm path length. Emission spectra were obtained with either a Perkin Elmer LS-50 spectrofluorometer, equipped with a Hamamatsu R928 phototube, or an Edinburgh FLS920 spectrofluorometer equipped with a Ge-detector for emission in the NIR spectral region. Correction of the emission spectra for detector sensitivity in the 550-1000 nm spectral region was performed by a calibrated lamp.<sup>26,27</sup> Emission quantum yields were measured following the method of Demas and Crosby<sup>28</sup> (standard used: [Ru(bpy)<sub>3</sub>]<sup>2+</sup> in air-equilibrated aqueous solution  $\Phi = 0.0407$  and HITCI, 1,1',3,3',3',3'-hexamethyl-indotricarbocyanine iodide, in EtOH  $\Phi = 0.308$ ). Emission intensity decay measurements in the range 10  $\mu$ s to 1 s were performed on a homemade time-resolved phosphorimeter. The estimated experimental errors are: 2 nm on the absorption and emission band maximum, 5% on the molar absorption coefficient and luminescence lifetime, and 10% on the luminescence quantum yield.

## RESULTS AND DISCUSSION

### Synthesis and structural characterization

Hydride-terminated silicon nanocrystals were prepared by thermal decomposition of hydrogen silsesquioxane (HSQ). Surface passivation, needed to prevent oxidation and aggregation of nanocrystals, was performed by room temperature hydrosilylation with chloro(dimethyl)vinylsilane (CDMVS) in the presence of diazonium salts (4-decyl diazobenzene tetrafluoroborate, 4-DDB) as radical initiators (step (i) in *Scheme 1a*).<sup>29</sup> This reaction introduces chlorosilane electrophilic groups on the surface of silicon nanocrystals, which can react with several nucleophilic reagents, such as Grignard reagents, alcohols, silanols and acetylides. We used a protected N-methylpropargylamine (step (ii) in *Scheme 1a*), that can be deprotonated by strong bases (e.g. LDA or n-BuLi) to obtain the corresponding acetylide.



**Scheme 1.** a) Three-step functionalization of SiNCs consisting in i) hydrosilylation step with chloro(dimethyl)vinyl silane (CDMVS), 4-decyldiazonium tetrafluoroborate (4-DDB), ii) functionalization with *N,N*-methyl-triphenylmethyl-propargyl amine (TPA), in presence of *N,N,N',N'*-tetramethylethylenediamine (TMEDA) and iii) deprotection with trifluoroacetic acid (TFA). b) Amidation of amine functionalised SiNCs with 1-pyrenebutyric acid (Py-COOH), in the presence of (1-cyano-2-ethoxy-2-oxoethylideneaminoxy)dimethylamino – morpholino – carbenium hexafluorophosphate (COMU), 1-ethyl-3-(3-dimethylaminopropyl)carbodiimide (EDC) and triethylamine (TEA) in dimethylformamide (DMF)

Triphenylmethyl group (better known as trityl group) was chosen<sup>30</sup> because it is stable under the nucleophilic and basic reaction conditions, it can be cleaved under mild conditions (addition of trifluoroacetic acid, TFA, that does not damage silicon nanocrystals) and the protection of the amine with this group is very easy (it involves *N*-methylpropargylamine and trityl chloride in the presence of a non-nucleophilic base such as triethylamine, TEA).

The steric hindrance of a bulky group as trityl has two main effects that need to be considered in optimising the reaction conditions: (i) trityl group can substitute only one of the two hydrogen atoms of a primary amine, such as propargylamine;<sup>30</sup> (ii) the protected amine is too bulky to cap all the chlorosilanes present on the surface of the silicon nanocrystals. As a consequence, unreacted chlorosilanes will be present on the surface of silicon nanocrystals and their presence is detrimental: while exposed at ambient moisture or alcohols used for the work up, they form silanols or silyl ethers that, in presence of acidic or basic catalysis, condense with each other, leading to aggregation of the nanocrystals through siloxane bridges. Therefore, we decided to cap the chlorosilanes by subsequent addition of an excess of *n*-BuLi nucleophile, as previously reported by us,<sup>24</sup> and to use a secondary amine, namely *N*-methylpropargylamine, to avoid deprotonation during reaction with excess *n*-BuLi.

The synthetic strategy, therefore, involves three different steps: (i) passivation of SiNCs with chlorosilane via radical initiated hydrosilylation; (ii) functionalisation with N,N-methyl-triphenylmethyl-propargyl amine; (iii) deprotection of the amine function promoted by acid (*Scheme 1a*). The so-obtained ammonium-terminated silicon nanocrystals are suspendable in polar solvents such as methanol (*Figure 4*).

Presence of primary and secondary amines on the SiNCs surface was detected by the ninhydrin test positive only after cleavage of the trityl group, and by  $^1\text{H-NMR}$  (See Experimental Section).



**Figure 4** – Vial containing a suspension of ammonium-terminated silicon nanocrystals in methanol under ambient (a) and 365 nm UV (b) light

We noticed that ammonium-terminated silicon nanocrystals are not dispersible in water if the counter anion is trifluoroacetate. Upon addition of HCl in methanol anion exchange takes place, replacing the trifluoroacetate with chloride. The so-obtained nanocrystals were suspendable in water. Ammonium-terminated silicon nanocrystals are proved to be cytotoxic.<sup>31</sup> Therefore, considering a potential biomedical application of those quantum dots, our research will be focussed on the linkage of a most biocompatible polymer (e.g. PEG) through amide bonds.

The possibility to further functionalise the so-obtained SiNCs via amide bond formation was tested by reaction with 1-pyrenebutyric acid in the presence of amide coupling reagents (1-cyano-2-ethoxy-2-oxoethylidenaminoxy)dimethylamino – morpholino – carbenium hexafluorophosphate and 1-ethyl-3-(3-dimethylaminopropyl)carbodiimide (COMU, EDC, as shown in *Scheme 1b*). The resulting SiNCs functionalised with pyrene chromophores was dispersed in DMF solution and the linkage of the chromophore was confirmed by photophysical characterisations (see below).

### Photophysical properties

The absorption spectrum of ammonium-terminated silicon nanocrystals in ethanol (line blue in *Figure 5*) exhibits the typical trend of alkyl-passivated SiNCs' absorption, which gradually increases at lower wavelengths.<sup>1</sup> The emission band (red line in *Figure 5*) is centred at about 750 nm with emission quantum yield of 24% and emission lifetime of 75  $\mu\text{s}$ .

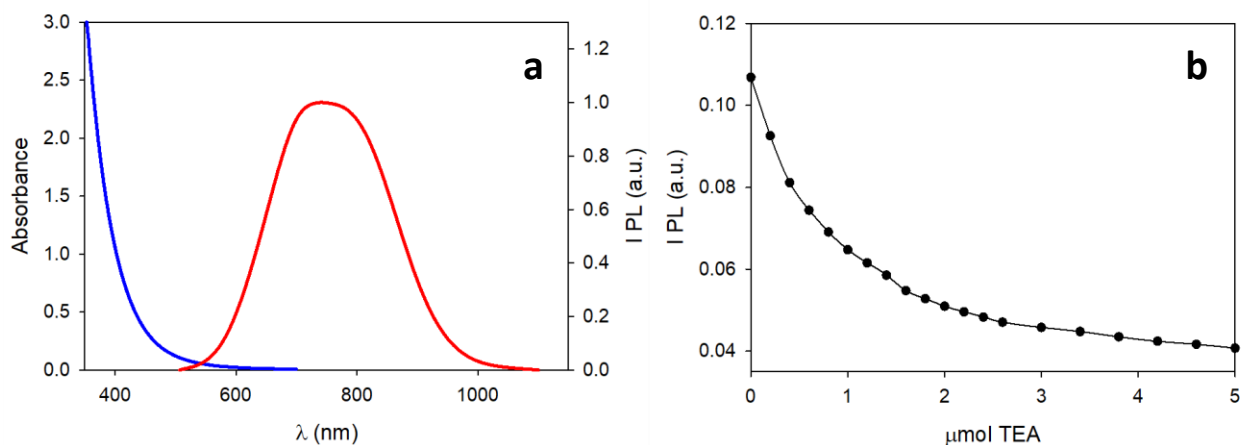


**Figure 5** – (a) Absorption (blue line) and emission (red line) of ammonium functionalised silicon nanocrystals in ethanol; (b) decay of the emission intensity upon addition of triethylamine (TEA)

Upon deprotonation of ammonium-terminated silicon nanocrystals with TEA in chloroform, the absorption and emission spectra maintained the same shapes, but a decrease of the emission intensity was observed (*Figure 5b*), corresponding to an emission quantum yield of 4%. This quenching process can be due to a photoinduced electron transfer between the silicon nanocrystal core and the terminal amine functionalities. The emission lifetime does not change significantly. This experimental finding is likely related to the fact that we cannot detect components shorter than 5  $\mu$ s with this experimental setup and the observed intensity decay is related to the emission of excitons formed in the inner part of the nanocrystal core, that are not affected by the photoinduced electron transfer process.

The absorption and emission spectra of water-suspended ammonium-terminated silicon nanocrystals are reported in *Figure 6*. The slight blue-shift observed in the photoluminescence (the emission band is centred at 675 nm) is probably due to an oxidation of the surface caused by a non-homogeneous coating of the surface.<sup>32</sup> The emission quantum yield was equal to 5% and the emission lifetime was about 50 microseconds.

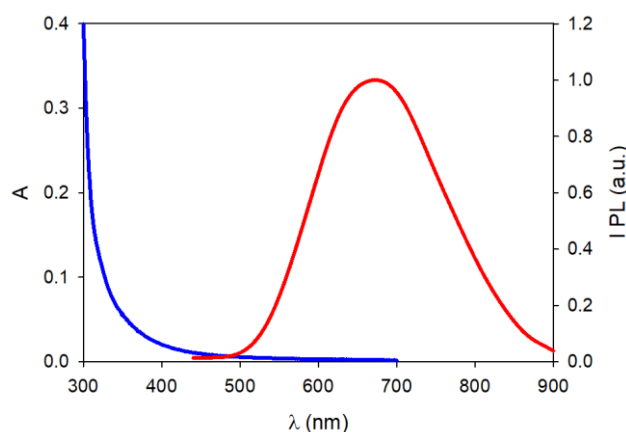


**Figure 6** – Absorption (blue line) and emission (red line) spectra of ammonium-terminated silicon nanocrystals in water

## Light-Harvesting Antenna

The absorption spectrum of **Si-Py** (blue line in *Figure 7*) displays a trend associated to the sum of the absorption of the silicon core (red line) and the 1-pyrenebutyric acid one (green line), demonstrating that no significant interaction takes place between the organic pyrene chromophore and the inorganic silicon core in the ground state.

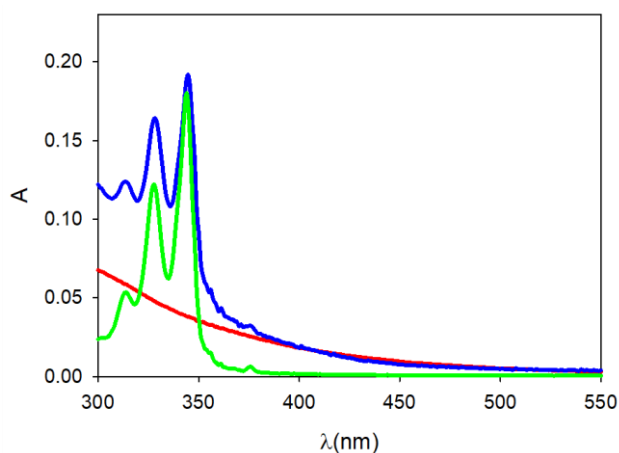


**Figure 7** – Absorption spectra of Si-Py (blue line), alkyl passivated silicon nanocrystals (in red) and 1-pyrenebutyric acid (green)

From these data, knowing the molar absorption coefficient for pyrenebutyric acid ( $3.7 \times 10^4 \text{ M}^{-1} \text{ cm}^{-1}$  at 344 nm, derived from spectrophotometric measurements) and the silicon core's one ( $1.0 \times 10^5 \text{ M}^{-1} \text{ cm}^{-1}$  computed at 430 nm,<sup>22</sup> where the absorption of the organic fluorophore does not occur) it is possible to estimate an average of 40 pyrene units per silicon nanocrystal.

Upon excitation at 450 nm where only the silicon core absorbs light, the characteristic red luminescence is present (*Figure 8a*) with a photoluminescence quantum yield of 1.4%, which is increased up to 11% ( $\tau = 20 \mu\text{s}$ ) upon addition of trifluoroacetic acid. This enhancement is compatible with protonation of amine groups that prevent photoinduced electron transfer processes, as previously discussed for ammonium-terminated silicon nanocrystals.

Upon excitation at 340 nm, where 70% of light is absorbed by pyrene and 30% of light by the silicon core the emission spectrum displays three main bands (*Figure 8b*) attributed to: (i) the pyrene monomer emission (380-420 nm, as confirmed by the emission spectrum of the 1-pyrenebutyric acid in blue); (ii) the emission of pyrene excimer (centred at about 480 nm); (iii) the silicon nanocrystal photoluminescence (from 600 nm), which is better observed using a time-gated detection (dashed line in *Figure 8b*).

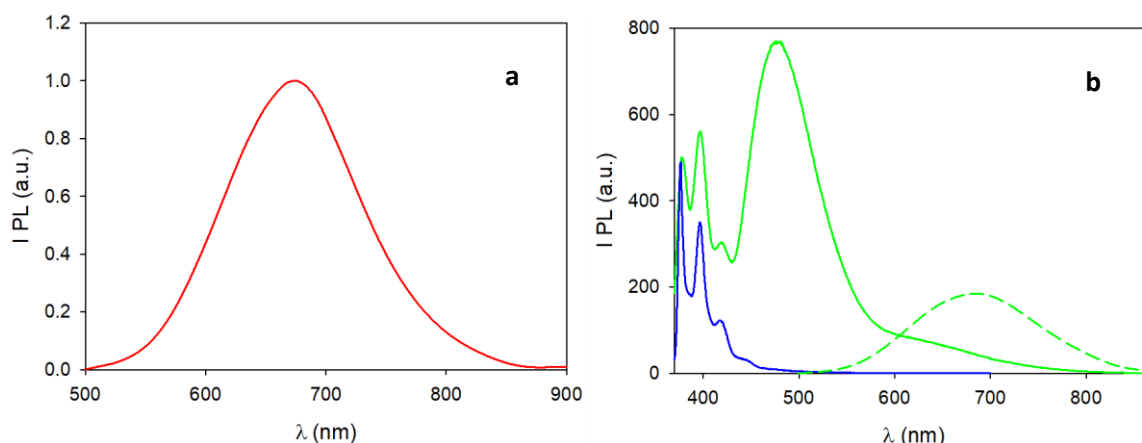


**Figure 8** – (a) Emission spectrum of silicon core upon excitation at 450 nm; (b) emission spectra of Si-py (green line) and 1-pyrenebutyric acid (blue line) in DMF exciting at 340 nm and emission of Si-py (green dashed line) with a time-gated detection of 50 microseconds (this emission is magnified)

The intense emission of the excimer is a proof of the high number of pyrene units linked to the nanocrystal, as previously observed for pyrene-functionalised nanocrystals.<sup>33</sup> On the other hand, the emission of pyrene monomer is strongly quenched (10-times). Indeed, the fluorescence lifetime of pyrene at 396 nm for **Si-Py** in air-equilibrated dimethylformamide solution is 3.7 ns, compared to 37 ns for 1-pyrenebutyric acid under the same experimental conditions. The same value (3.7 ns) corresponds to the rise time in SiNCs PL emission at 700 nm upon excitation at 340 nm, which proves the occurrence of energy transfer from pyrenes to the silicon core.

A further demonstration of the energy transfer between the organic chromophores and the silicon core is given by the excitation spectrum recorded at 700 nm (blue line in Figure 9), where only the nanocrystal contributes to the emission. The excitation spectrum shows a good match with the absorption spectrum (red line in Figure 9).

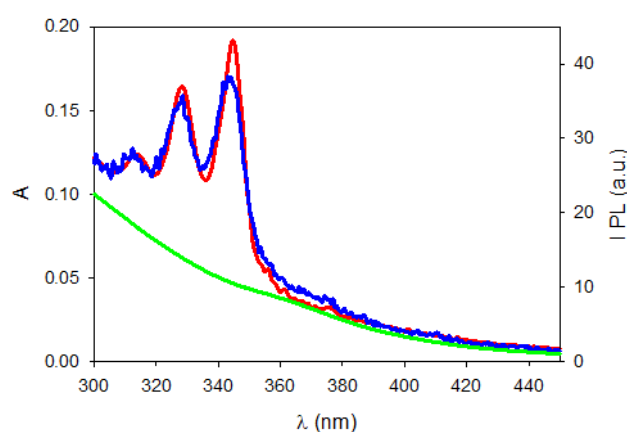


**Figure 9** – Absorption (red line) and excitation spectra (blue line,  $\lambda_{em} = 700$  nm, time gated detection with delay = 50  $\mu$ s and gate time = 1 ms) of **Si-Py** in DMF. For comparison purpose, the excitation spectrum (green line) of a physical mixture of 1-pyrenebutyric acid and ammonium-terminated SiNCs is reported under the same experimental conditions.

The close match of the absorption (red line in Figure 9) and excitation spectra (blue line in Figure 9) proves the occurrence of energy transfer with efficiency higher than 90%. The excitation spectrum was also measured for ammonium-terminated silicon nanocrystals mixed with free 1-pyrenebutyric

acid in the appropriate ratios to match the **Si-Py** absorbance profile. In this case, the excitation spectrum (green line in *Figure 9*) is superimposed to the absorption spectrum of the ammonium-terminated SiNC sample and no contribution from the pyrene chromophores is present. As previously observed,<sup>13,33</sup> in the physical mixture, excitation of pyrene does not result in sensitised emission of the SiNC: pyrene fluorescent excited state is short lived (tens of ns) and cannot interact with non-covalently bound SiNCs present in low concentration.

## CONCLUSIONS

We have successfully synthesized red/NIR emitting amine-terminated silicon nanocrystals characterized by high emission quantum yield and long emission lifetimes, using a three-step synthetic strategy that involves a bulky protecting group cleavable in mild conditions. These SiNCs are colloidally stable in several polar solvents, such as ethanol. Upon protonation, ammonium-terminated silicon nanocrystals with chloride counter anions are obtained and they can be suspended in water.

The amine-terminated SiNCs can be post-functionalised via formation of amide bond, fairly stable under physiological conditions. We demonstrated a successful post-functionalization with pyrene chromophore through amidation. The resulting hybrid system works as a light-harvesting antenna stable in a polar environment: upon UV excitation of the pyrene chromophores, sensitised red emission of the silicon core is observed via an efficient energy transfer process. The amidation reaction needs much lower amount of chromophore, compared to previously published procedures: this result is important in view of future implementation with more sophisticated and expensive chromophores. Furthermore, the same amidation approach can be used to append PEG polymers and proteins, as currently under investigation in our laboratory.

## CONFLICTS OF INTERESTS

There are no conflicts of interest to declare.

## ACKNOWLEDGMENTS

The University of Bologna is gratefully acknowledged.

## REFERENCES

- 1 R. Mazzaro, F. Romano and P. Ceroni, *Phys. Chem. Chem. Phys.*, 2017, **19**, 26507–26526.
- 2 B. F. P. Mcvey and R. D. Tilley, *Acc. Chem. Res.*, 2014, **47**, 3045–3051.
- 3 J. Park, L. Gu, G. Von Maltzahn, E. Ruoslahti, N. Sangeeta and M. J. Sailor, *Nat Mater*, 2009, **8**, 331–336.
- 4 S. Chinnathambi, S. Chen and S. Ganesan, *Adv Heal. Mater.*, 2014, **3**, 10–29.
- 5 M. Montalti, A. Cantelli and G. Battistelli, *Chem. Soc. Rev.*, 2015, **44**, 4853–4921.
- 6 X. Ji, H. Wang, B. Song, B. Chu and Y. He, *Front. Chem.*, 2018, **6**, 1–9.
- 7 F. Erogbogbo, K.-T. Yong, I. Roy, R. Hu, W.-C. Law, W. Zhao, H. Ding, F. Wu, R. Kumar, M. T. Swihart and P. N. Prasad, *ACS Nano*, 2011, **5**, 413–423.

- 8 M. A. Islam, H. Mobarok, R. Sinelnikov, T. K. Purkait and J. G. C. Veinot, *Langmuir*, 2017, **33**, 8766–8773.
- 9 L. Ravotto, Q. Chen, Y. Ma, S. A. Vinogradov, M. Locritani, G. Bergamini, F. Negri, Y. Yu, B. A. Korgel and P. Ceroni, *Chem*, 2017, **2**, 550–560.
- 10 E. J. New, D. Parker, D. G. Smith and J. W. Walton, *Curr. Opin. Chem. Biol.*, 2010, **14**, 238–246.
- 11 A. J. Amoroso and S. J. A. Pope, *Chem Soc Rev*, 2015, **44**, 4723–4742.
- 12 L. Sun, R. Wei, J. Feng and H. Zhang, *Coord. Chem. Rev.*, 2018, **364**, 10–32.
- 13 M. Locritani, Y. Yu, G. Bergamini, M. Baroncini, J. K. Molloy, B. A. Korgel and P. Ceroni, *J. Phys. Chem. Lett.*, 2014, **5**, 3325–3329.
- 14 A. Fermi, M. Locritani, D. Carlo, M. Pizzotti, S. Caramori, Y. Yu, B. A. Korgel and P. Ceroni, 2015, 481–495.
- 15 F. Romano, Y. Yu, B. A. Korgel, G. Bergamini and P. Ceroni, *Top. Curr. Chem.*, 2016, **374**, 89–106.
- 16 S. Chatterjee and T. K. Mukherjee, *J. Phys. Chem. C*, 2013, **117**, 10799–10808.
- 17 J. H. Warner, A. Hoshino, K. Yamamoto and R. D. Tilley, *Angew Chemie Int. Ed.*, 2005, **44**, 4550–4554.
- 18 G. B. De los Reyes, M. Dasog, M. Na, L. V. Titova, J. G. C. Veinot and F. A. Hegmann, *Phys. Chem. Chem. Phys*, 2015, **17**, 30125–30133.
- 19 M. Dasog, Z. Yang, S. Regli, T. M. Atkins, A. Faramus, M. P. Singh, E. Muthuswamy, S. M. Kauzlarich, R. D. Tilley and J. G. C. Veinot, *ACS Nano*, 2013, **7**, 2676–2685.
- 20 A. N. Thiessen, T. K. Purkait, A. Faramus and J. G. C. Veinot, *Phys. Status Solidi Appl. Mater. Sci.*, 2018, **215**, 1–5.
- 21 R. J. Clark, M. Aghajamali, C. M. Gonzalez, L. Hadidi, M. A. Islam, M. Javadi, H. Mobarok, T. K. Purkait, C. J. T. Robidillo, R. Sinelnikov, A. N. Thiessen, J. Washington, H. Yu and J. G. C. Veinot, *Chem Mater*, 2017, **29**, 80–89.
- 22 M. R. . Hessel, C. M.; Reid, D.; Panthani, M. G.; Rasch and B. A. Goodfellow, B. W.; Wei, J.; Fujii, H.; Akhavan, V.; Korgel, *Chem. Mater*, 2012, **24**, 393–401.
- 23 I. M. D. Höhle, J. Kehrlé, T. K. Purkait, J. G. C. Veinot and B. Rieger, *Nanoscale*, 2015, **7**, 914–918.
- 24 R. Mazzaro, A. Gradone, S. Angeloni, G. Morselli, P. G. Cozzi, F. Romano, A. Vomiero and P. Ceroni, *ACS Photonics*, 2019, **6**, 2303–2311.
- 25 M. Friedman and L. D. Williams, *Bioorg. Chem.*, 1974, **3**, 267–280.
- 26 M. Montalti, A. Credi, L. Prodi and M. T. Gandolfi, *Handbook of photochemistry*, 2006.
- 27 V. Balzani, P. Ceroni and A. Juris, *Photochemistry and Photophysics - Concepts, Research, Applications*, 2015.
- 28 G. A. Crosby and J. N. Demas, *J. Phys. Chem.*, 1971, **75**, 991–1024.

- 29 I. M. D. Höhle, J. Kehrle, T. Helbich, Z. Yang, J. G. C. Veinot and B. Rieger, *Chem. - A Eur. J.*, 2014, **20**, 4212–4216.
- 30 P. G. M. Wuts, in *Greene's Protective Groups in Organic Synthesis*, 2014, pp. 1086–1087.
- 31 S. Bhattacharjee, L. H. J. De Haan, N. M. Evers, X. Jiang, A. T. M. Marcelis, H. Zuilhof, I. M. C. M. Rietjens and G. M. Alink, *Part. Fibre Toxicol.*, 2010, **7**, 1–12.
- 32 R. Sinelnikov, M. Dasog, J. Beamish, A. Meldrum and J. G. C. Veinot, *ACS Photonics*, 2017, **4**, 1920–1929.
- 33 R. Mazzaro, M. Locritani, J. K. Molloy, M. Montalti, Y. Yu, B. A. Korgel, G. Bergamini, V. Morandi and P. Ceroni, *Chem. Mater.*, 2015, **27**, 4390–4397.